European Journal of Molecular & Clinical Medicine

ISSN 2515-8260 Volume 9, Issue 7, Summer 2022

AUTOMATED LUNG CANCER DIAGNOSIS USING PRE-TRAINED DEEP NEURAL ARCHITECTURES

[1]V Anantha Natarajan, [2]M Sunil Kumar, [3]T Naresh
[1,2]School of Computing, Department of CSE, Mohan Babu University, AP, India.
[3]Aditya Institute of Technology and Management, Tekkali, AP, India.
Email: vananthanatarajan@vidyanikethan.edu

ABSTRACT

Uncontrolled cell proliferation in lung tissues is what is known as lung cancer. Early Lung Cancer detection may hold the key to the disease's recovery. This research examines non-invasive techniques to aid with nodule detection. From the Computer Tomography (CT) pictures, it provides a Computer Aided Diagnosis System (CAD) for the early diagnosis of lung cancer nodules. The use of CAD systems aids radiologists in providing more accurate diagnoses when interpreting images. This method's main objective is to develop a CAD system for classify the nodule and using computed Tomography images to classify the lung cancer. In order to determine the optimal treatment plan for patients and their possibility of survival, convolutional neural networks can more quickly and reliably recognize and classify various kinds of lung cancer. The benign tissue, adenocarcinoma, big cell carcinoma, and squamous cell carcinoma are all considered in this work.

Keywords: cancer detection, computer aided diagnosis, cancer nodules, convolutional neural networks, benign tissue, large cell carcinoma, squamous carcinoma, adenocarcinoma.

INTRODUCTION

The most prevalent type of cancer and the main reason for cancer-related deaths worldwide is lung cancer. Lung cancer is the cause of 5.9% of cancer cases and 8.1% of cancer-related deaths in India [1]. Squamous and small cell lung cancer histologic forms, which are highly related with tobacco use, used to dominate the epidemiology of lung cancer in India. Later, adenocarcinoma began to replace them, and currently it is the predominant histologic type. In order to screen for lung cancer, low-dose computed tomography (LDCT) of the chest is a well-established method. Nevertheless, India lacks a formal lung cancer screening program despite having a sizable lung cancer burden. The widespread implementation of LDCT screening has been hampered by problems like cost, logistical limitations, and worries about high false-positive rates because of the high prevalence of tuberculosis. Lung nodules seen during LDCT screening are frequently characterized using PET-computed tomography (CT). However, due to infectious circumstances restricting its usage, PET-CT [2] may have a high false-positive rate in poor nations like India.

Lung cancer patients typically undergo noninvasive imaging staging to determine the disease's local and global extent. In patients with treatable illness, noninvasive staging is very crucial. The most accurate technique for staging lung cancer noninvasively is a whole-body PET-CT scan. However, a radionuclide bone scan is paired with a contrast-enhanced CT scan of the chest and upper abdomen (containing the liver and adrenals) for staging in locations where PET-CT is not easily accessible. The goal of this study is to create a computer-aided design (CAD) system for early lung cancer detection based on an automatic identification of the lung areas seen in chest computed tomography (CT) images. The following are some challenges to finding lung nodules on radiographs:

- Nodules have a wide range of densities, which impacts how well they can be seen on radiographs; some nodules are barely denser than the lung tissue around them, while the highest density ones are calcified.

- Nodules can form anywhere within the lung field and can be hidden by ribs and structures below the diaphragm, giving the lung field a wide range of contrast.

This paper aims to suggest a Computer Aided Diagnosing (CAD) system for Detection of Lung Nodules as a solution to these issues. The five primary components of this system are the pre-processing of the CT images, segmentation of the lung region, identification of lung nodules, analyze the segmented area, and classification of the cancer kind. The effectiveness of a CAD system rests on its ability to enhance radiologists' clinical practice in

identifying substantial lung nodules. Although the FDA has approved two commercial CADe systems for the identification of lung nodules in CT scans since 2004, there hasn't yet been a large-scale prospective clinical research to assess the efficacy of CADe systems in everyday clinical practice. Numerous investigations on the performance of retrospective observers have been done so far. The same characteristics that affect computerized detection also affect radiologists' ability to detect lung nodules on CT scans, in addition to other clinical criteria that are not taken into account in laboratory observer studies. Therefore, it may not be possible to extrapolate from the relative capabilities of the radiologists with and without CAD in these trials with a small data set to their efficiency in clinical situations.

LITERATURE SURVEY

The widespread use of LDCT screening methods has resulted in a massive increase in CT scans, which has placed a heavy pressure on radiologists. Massive CT scan manual analysis is turning into a highly laborious and time-consuming operation. Therefore, an effective Computer-Aided Diagnosis (CAD) system is required to assist the process of automatically evaluating a large number of CT images in order to reduce the radiologist's burden. CAD systems have been routinely used in recent years to treat many different disorders [3]. A standard CAD system can be divided into a detection system (CADe) and a diagnostic system in particular (CADx). The goal of CADe is to identify the interest regions of lung CT scans in order to find abnormal lesions. The purpose of CADx is to help doctors or radiologists identify the kind and malignancy of abnormalities. A CAD system for lung cancer typically focuses on candidate nodule detection, false positive reduction, and nodule classification, with the first three steps being preprocessing, nodule detection, and nodule classification.

Preprocessing is mostly done to standardize the data, decrease noise, and segment the lung's Regions of Interest (ROI) for a more focused search for pulmonary nodules. Candidate nodules should be found as many times as possible during the nodule detection stage, which frequently produces high sensitivity and low accuracy. To detect accurate nodular marks, the false positive reduction step should then be carried out. The categorization stage's final goal is to foretell the likelihood of nodule malignancy [4]. It has been used to enhance the functionality of CAD systems for pulmonary nodule analysis in numerous published papers.

Conventional classification techniques such multiple gray-level thresholding, linear discriminant analysis, distance transformation, and Support Vector Machine (SVM) are frequently used by researchers to quickly investigate lung nodules when resources and datasets are limited [5]–[10]. CNN, U-Net, R-CNN, RPN, and ResNet, and Retina-Net are the most often utilized network topologies for nodule detection.

In order to discover candidates using bounding boxes, Wang et al. [11] presented a nodule-size-adaptive model that is comparable to Faster R-CNN. Bi-directional ConvLSTM U-Net with Densely Connected Convolutions (BCDUNet), created by Azad et al. [12], uses several concatenation techniques to fully use numerous feature maps for lung nodule segmentation and recognition. Additionally, in order to combine the power of several networks, some fusion networks are also investigated employing multi-stream topologies [13], [14], [15]-[17]. In order to create 3D Gaussian blob nodules, Liu et al. [80] used three identical 3D ResUNets. The network was then tweaked by adding 3D RPN heads, which led to increased sensitivity on big nodules.

The classification of nodules is the last stage in CAD systems. Most CAD systems are made to predict nodule malignancy and determine whether a nodule is malignant, although some are made to classify different types of nodules [8], [20]. In this stage, a variety of classification approaches are used: (1) conventional classifiers, such as Support Vector Machines, instance based classifiers, probabilistic classifiers, ensemble classifiers, and optimal linear classifiers [[21]; (2) advanced state of art CNNs [22]; (3) CNNs combined with support vector classifiers or tree based classifiers [23], [24], [25]; (4) multi-stream heterogeneous CNNs. To extract numerous features from nine planes and determine the malignancy of nodules, Xie et al. [26] used a 3D multi-view knowledge-based collaborative (MV-KBC) deep model that was constructed with three pre-trained ResNet-50 networks[34][28].

METHODOLOGY

CNNs have had a substantial impact on the development of CAD and significantly increase the accuracy of nodule identification and classification jobs[27][29]. CNNs are made primarily in an end-to-end fashion to identify the underlying relationships between images and dynamically extract the most descriptive features. Convolutional,

pooling, and fully connected layers, as well as activation functions, are frequently used to construct CNNs[33][35]. The fully connected layers map the retrieved features to the output while the convolution and pooling layers extract features[30][31]. Additionally, a particular activation function, such as sigmoid, softmax, or ReLU, follows each completely linked layer. Characteristics of data and classification tasks are taken into consideration while choosing the activation functions. To process images, classical approaches still use a number of computer vision techniques. The determination of hand-crafted features and the manual selection of the significant ones in each image required for feature extraction mainly rely on the researchers' subjective assessment[36][32].

This study utilizes the transfer learning approach for training CNN models used for classifying the lung nodules. An algorithm that saves knowledge obtained while completing one job and may be applied to another activity that is similarly related is known as a transfer learning algorithm. It is possible to somewhat increase the effectiveness and accuracy of CAD systems by initializing or fine-tuning models using pre-trained CNNs.

Dataset

The largest reference database for lung nodules that is open to the public is the Lung Image Database Consortium and Image Database Resource Initiative (LIDC-IDRI). This database includes 1018 CT images together with XML files that correspond to two-phase picture annotations made by four seasoned radiologists. Nodule traits, kinds, and position are also included in the annotation [38].

Preprocessing

Preprocessing is an important first step in the analysis of lung CT scans since the raw pictures' abundance of irrelevant information affects a CAD system's productivity and diagnostic precision. The key searching area for doing nodule detection is the major lung volume, or ROI. Therefore, the main objectives in this stage are to remove distracting elements like lung tissues and image artefacts, as well as to recover or enhance useful information. As a preprocessing phase in a CAD system, it is demonstrated that adjusting lung segmentation algorithms can help prevent missing nodules by 5% to 17% [39].

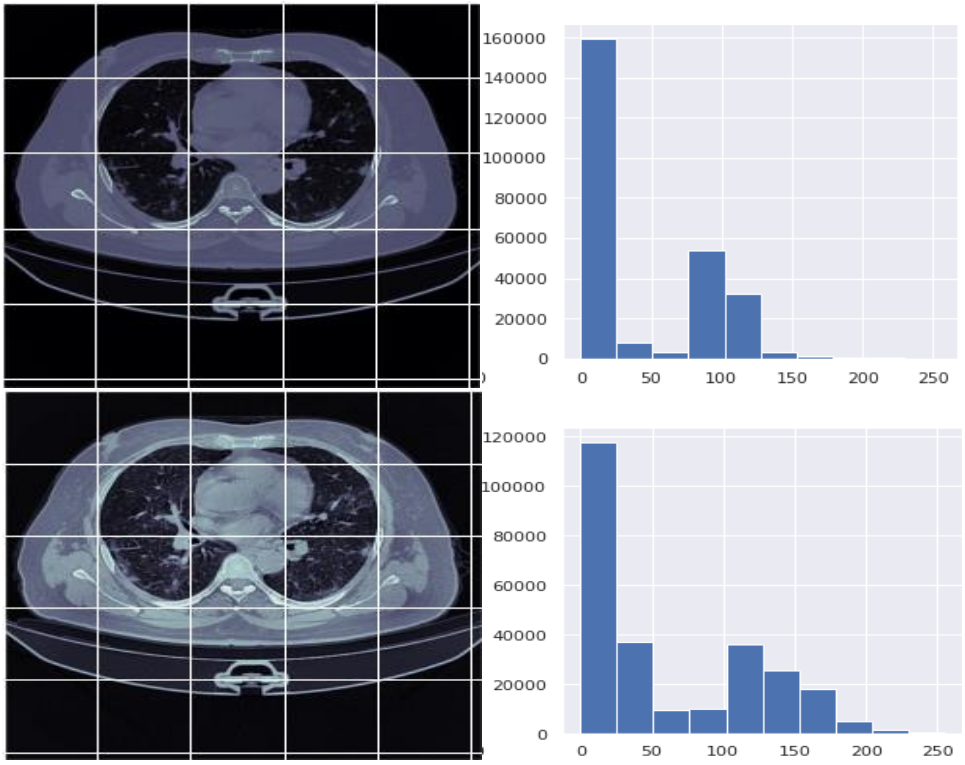

Fig. 1 Original CT image and Contrast enhanced CT image

In order to lessen the issue of noise amplification, Contrast Limited AHE (CLAHE), a form of adaptive histogram equalization, limits the contrast amplification. [40] The gradient of the transformation function determines the contrast enhancement in CLAHE near a given pixel value. This is proportional to the histogram's value at that pixel value and the gradient of the neighbourhood cumulative distribution function (CDF). Before calculating the CDF, CLAHE clips the distribution at a predetermined value to reduce the amplification. As a result, the transformation function's transformation function's slope is constrained. The normalization of the histogram and, consequently, the area of the neighbourhood region, determine the threshold at which the histogram is clipped. The resulting amplification is typically limited to between 3 and 4. It is preferable to evenly distribute the portion of the distribution that surpasses the clip limit throughout all histogram bins rather than toss it out. As a result of the redistribution, some bins will once more cross the clip limit, resulting in a practical clip limit that is higher than the legal limit and whose precise value relies on the image. If this is not what is desired, the redistribution process can be repeated until the excess is little.

Segmentation

The delineation of lung structures is the initial stage of preprocessing after reading the CT scan because it is evident that the areas of interest are located inside the lungs. The darker areas on the CT scans are clearly the lungs. The veins or air are located in the bright area inside the lungs. As a result of research showing that it is effective, a cutoff of 604(-400 HU) is utilized everywhere. In order to preserve the potential region of interest related to the lung wall, we segment the structures of the lungs from each slice of the CT scan image. Several nodules could be anchored to the bronchial wall. To segment the lung from the rat CT slice as a first step convert the image in to binary form and remove the large connected regions attached to the border of an image. Perform an erosion with a diameter of 4 to separate the lung nodules. Then perform a closure operation with a diameter of 20 to keep the nodules attached to the lung wall. In the binary mask of lungs fill the small holes. Extract the lung region by superimposing the binary mask on the raw input image.

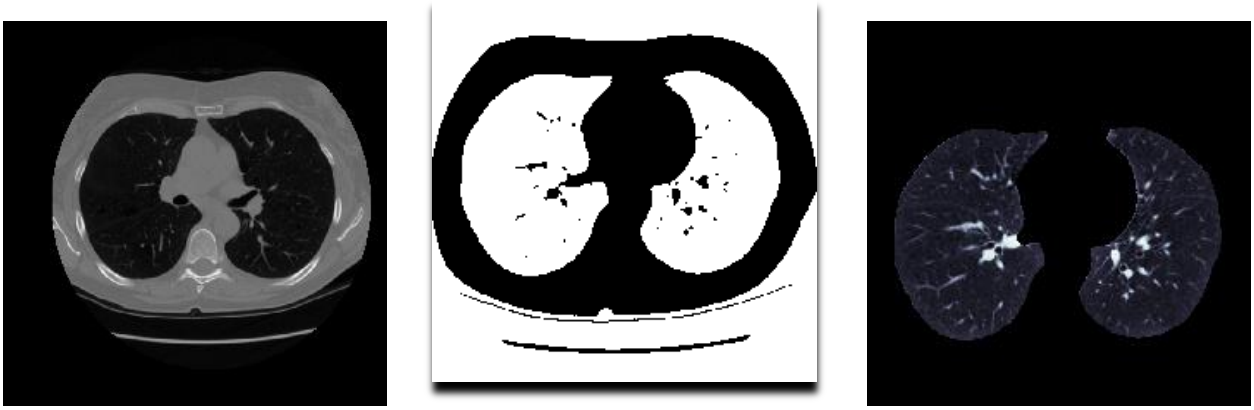

Fig. 2 Original Image, Processed image, and segmented lung

Since the search space is relatively broad, the next challenge is to identify candidate locations containing nodules after fragmenting the lung structures from the CT-scanned images. Due to computational limitations, the entire image cannot be classified using 3D CNNs; instead, potential cancerous spots must be located and then classified. Experiments revealed that the intensity in every location of interest was greater than 604 (-400 HU). The darker parts are filtered using this threshold. This drastically lowers the number of possibilities while maintaining all the significant regions with good recall. After that, classify every candidate point to lower the number of false positives.

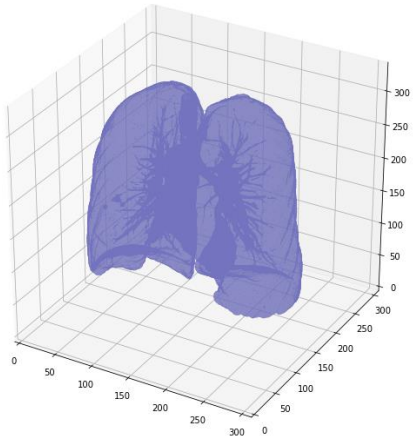

Fig. 3 Projection of segmented lung in to 3D space

Classification

Using the transfer learning approach the parameters discovered during the model's training in one domain can be applied to a problem in another, more recent or unexplored domain. For the purpose of solving picture categorization and other computer vision applications, there are currently many pre-trained models available. Three of the more well-known models are the VGG, the GoogLeNet, and the residual network. These pre-trained models are widely employed in transfer learning tasks because they are thought to be more effective and reliable. Inception v3, a model with symmetric-asymmetric construction pieces, Resnet-50, and VGG-16/19, known as the first explicit deep architecture with several layers, are used in this study.

Inception V3's architecture design is different from that of its predecessors in that it places a strong emphasis on minimizing computational complexity. When compared to VGG networks, inception models are generally more effective in terms of the amount of learnable parameters and the consumption of resources (storage and other resources). The computational effectiveness of the inception network must not be impacted by attempts to restructure or improve it. If not, it will be difficult to adapt the modified model to new applications. The accompanying schematic design (Fig. 4) illustrates the architecture of an Inception v3 network, which comprises the following crucial elements: factorized convolutions, smaller convolutions, asymmetric convolutions, and an auxiliary classifier.

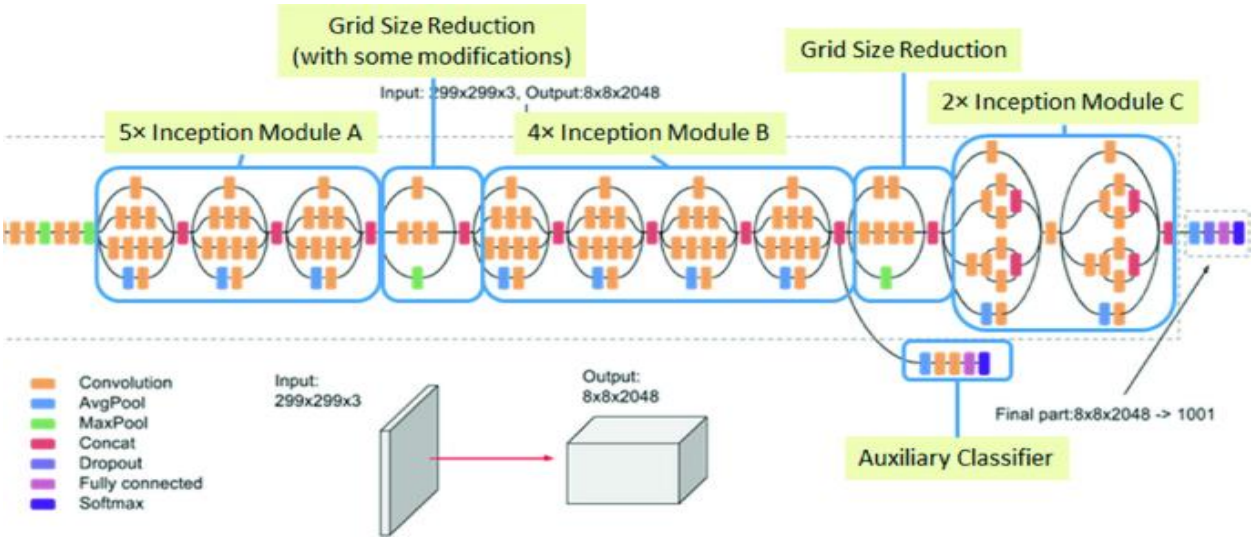

Fig. 4 Architecture of Inception V3 [38]

Longer training times are needed for deep neural networks, and overfitting is likely. A residual learning strategy was put out to solve these problems and shorten the training period for models that are substantially deeper than traditional neural models. The accuracy approaches a saturation point during neural training and tends to decline if model training is extended. The name for this is the "degradation problem." This shows that different neural network topologies have different properties. ResNet follows residual mapping is used to solve this issue. The residual network allows for explicit mapping of residuals rather than relying on the assumption that layer stacking will be sufficient to transfer an input to an output. In Fig. 5, the fundamental elements of a residual network are depicted.

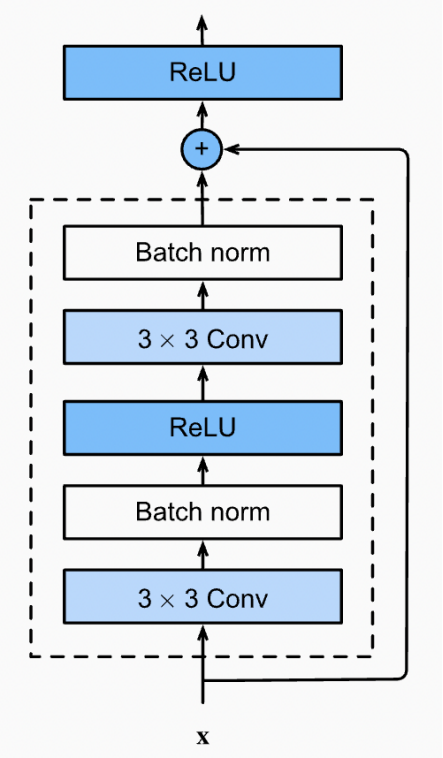

Fig. 5 Architecture of Inception V3 [39]

A variation of the CNN architecture known as VGG16 is one of the most effective deep neural models (shown in Fig. 6). The use of convolutional layers with 3x3 size filters and a maximum pooling with 2x2 size filters is a significant and distinctive feature of VGG16. In the architecture, the convolution and max pooling layers are positioned consistently. Two completely connected layers with softmax activation make up the categorization layer. There are 138 million trainable parameters in the network overall.

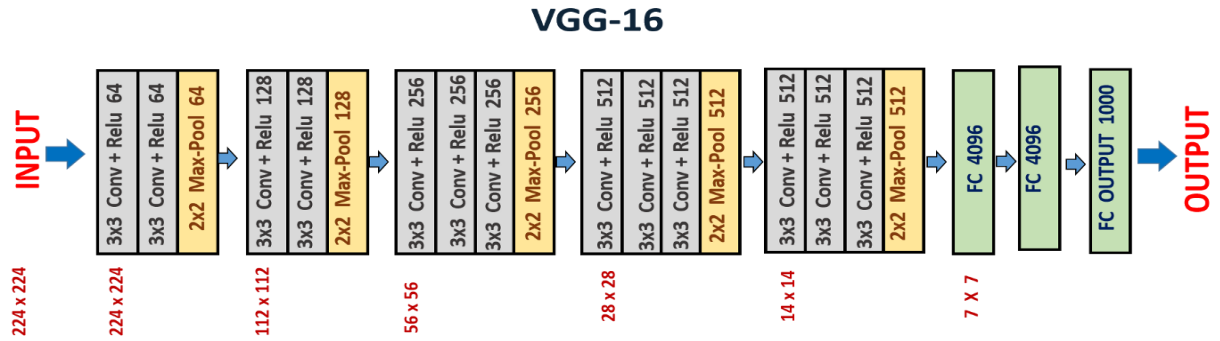

Fig. 6 Architecture of VGG-16 model [40]

RESULTS AND ANALYSIS

A commonly available lung CT images from the dataset stated in the previous section is used to assess the effectiveness of the suggested lung image feature extraction and classification method. 1018 photos were available in the dataset that is used to train and test deep learning models. The images are segmented after first being adjusted. The models are trained using segmented images from the lung region of the CT scans (VGG-16, Resnet50, and Inception v3). Although they were trained on the Imagenet dataset, pre-trained models were employed as feature extractors. The images were then categorized as either large cell, small cell, squamous, or normal lung images using fully connected neural layers. A grid search procedure was used to adjust the hyperparameters.

Table 1. Summary of Performance of model with RMSProp optimization

Epoch	VGG-16		RESNET-50		Inception-v3	
	Train	Test	Train	Test	Train	Test
1	0.36576	0.48092	0.47433	0.28963	0.46099	0.62107
10	0.66099	0.7044	0.61718	0.49796	0.81909	0.84077
20	0.76385	0.66842	0.67052	0.71577	0.91084	0.91463
30	0.78099	0.82751	0.65337	0.69304	0.91242	0.92599
40	0.85147	0.85781	0.69147	0.71008	0.94099	0.94115
50	0.86671	0.8919	0.73147	0.74796	0.91623	0.91842
60	0.89147	0.88433	0.69147	0.70819	0.95242	0.93925
70	0.89147	0.90137	0.72004	0.77448	0.96385	0.95819
80	0.88004	0.88054	0.69718	0.75365	0.95623	0.95251
90	0.90099	0.88433	0.7429	0.77448	0.94671	0.96008
100	0.92766	0.92789	0.74671	0.74418	0.93909	0.91274

The ideal number of epochs was chosen based on the average validation loss across 05 folds, and Tables 1 and 2 summarize the model accuracy attained for various epochs. After the 100th epoch, the VGG-16 provide an accuracy of 96% using the ADAM optimization algorithm. Although the VGG model can boost its accuracy by adding more layers, if the number of layers exceeds 20, it is unable to converge to global minima. Because of the vanishing gradient problem and declining learning rate, the model weights are not updated. Batch normalizing is used to control gradient explosion. The residual learning network can be used to limit the vanishing and gradient problem (RESNET-50). However, given that the stochastic gradient descent optimization technique was utilized in the RESNET's first implementation, it is clear from the tabulated data that the network performs poorly. The SGD with a learning rate scheduler may perform better than the ADAM algorithm because the latter has difficulties convergent to the best solution.

Table 2. Summary of Performance of model with RMSProp optimization

Epoch	VGG-16		RESNET-50		Inception-v3	
	Train	Test	Train	Test	Train	Test
1	0.29622	0.28676	0.29812	0.19017	0.32479	0.43828
10	0.43146	0.44017	0.50955	0.49509	0.63336	0.66934
20	0.48289	0.49131	0.51336	0.62956	0.70193	0.71479
30	0.50003	0.50835	0.5705	0.66365	0.73431	0.74131
40	0.51717	0.5254	0.61241	0.68638	0.7705	0.79812
50	0.5305	0.5235	0.63908	0.67502	0.8086	0.80191
60	0.53622	0.52729	0.60289	0.711	0.80289	0.81706

70	0.53241	0.54623	0.61431	0.7129	0.84289	0.82464
80	0.54003	0.54812	0.62574	0.70532	0.83717	0.83221
90	0.55146	0.53297	0.6505	0.69585	0.85622	0.82653
100	0.54955	0.57843	0.65622	0.73941	0.86003	0.82653

CONCLUSION

Lung cancer is on the rise, thus pathologists and doctors need a support system like computer-aided diagnosis to make diagnoses and administer treatments quickly. This study examines the capabilities and restrictions of various optimization methods as well as how well they function when used with trained models. The use of ADAM optimization has been found to help models like the VGG-16 and Inception v3 achieve improved accuracy, however the RESNET model does not converge to an optimal solution when using either the ADAM or the RMSprop algorithm. Despite the proposed method's excellent performance, it would be beneficial to test it with more photos from different databases. In order to more properly assess the model's performance, we intend to incorporate more photos while training the model from scratch in the future. These models could be utilized to deliver fast diagnostics and saved in the cloud. The effort required of the clinician should be greatly reduced. Future research will concentrate on gathering regional CT scans of lung cancer cases and using them to assess the trained models.

REFERENCES

1. Garg, Avneet, et al. "Evaluation of delays during diagnosis and management of lung cancer in India: A prospective observational study." *European Journal of Cancer Care* 31.5 (2022): e13621.
2. Nomura, Kotaro, et al. "Diagnostic value of nodal staging of lung cancer with usual interstitial pneumonia using PET." *The Annals of Thoracic Surgery* (2022).
3. S. Cressman, ‘‘The cost-effectiveness of high-risk lung cancer screening and drivers of program efficiency,’’ J. Thoracic Oncol., vol. 12, no. 8, pp. 1210–1222, Aug. 2017.
4. I. Sluimer, A. Schilham, M. Prokop, and B. van Ginneken, ‘‘Computer analysis of computed tomography scans of the lung: A survey,’’ IEEE Trans. Med. Imag., vol. 25, no. 4, pp. 385–405, Apr. 2006.
5. P. P. R. Filho, A. C. D. S. Barros, G. L. B. Ramalho, C. R. Pereira, J. P. Papa, V. H. C. de Albuquerque, and J. M. R. S. Tavares, ‘‘Automated recognition of lung diseases in CT images based on the optimum-path forest classifier,’’ Neural Comput. Appl., vol. 31, no. 2, pp. 901–914, Feb. 2019.
6. H. Han, L. Li, F. Han, B. Song, W. Moore, and Z. Liang, ‘‘Fast and adaptive detection of pulmonary nodules in thoracic CT images using a hierarchical vector quantization scheme,’’ IEEE J. Biomed. Health Informat., vol. 19, no. 2, pp. 648–659, Mar. 2015.
7. M. Bergtholdt, R. Wiemker, and T. Klinder, ‘‘Pulmonary Nodule Detection Using a Cascaded SVM Classifier,’’ in Computer-Aided Diagnosis, vol. 9785, G. D. Tourassi and S. G. Armato, Eds. Bellingham, WA, USA: SPIE, 2015.
8. S. G. and J. P., ‘‘A fully-automated system for identification and classification of subsolid nodules in lung computed tomographic scans,’’ Biomed. Signal Process. Control, vol. 53, Aug. 2019, Art. no. 101586.
9. S. M. Naqi, M. Sharif, and I. U. Lali, ‘‘A 3D nodule candidate detection method supported by hybrid features to reduce false positives in lung nodule detection,’’ Multimedia Tools Appl., vol. 78, no. 18, pp. 26287–26311, Sep. 2019.
10. M. S. Brown, P. Lo, J. G. Goldin, E. Barnoy, G. H. J. Kim, M. F. McNittGray, and D. R. Aberle, ‘‘Toward clinically usable CAD for lung cancer screening with computed tomography,’’ Eur. Radiol., vol. 24, no. 11, pp. 2719–2728, Nov. 2014.
11. J. Wang, J. Wang, Y. Wen, H. Lu, T. Niu, J. Pan, and D. Qian, ‘‘Pulmonary nodule detection in volumetric chest CT scans using CNNs-based Nodule-Size-Adaptive detection and classification,’’ IEEE Access, vol. 7, pp. 46033–46044, 2019.

12. R. Azad, M. Asadi-Aghbolaghi, M. Fathy, and S. Escalera, ‘‘Bidirectional ConvLSTM U-Net with densley connected convolutions,’’ in Proc. IEEE/CVF Int. Conf. Comput. Vis. Workshop (ICCVW), Oct. 2019, pp. 406–415.
13. S. Chen, J. Qin, X. Ji, B. Lei, T. Wang, D. Ni, and J.-Z. Cheng, ‘‘Automatic scoring of multiple semantic attributes with multi-task feature leverage: A study on pulmonary nodules in CT images,’’ IEEE Trans. Med. Imag., vol. 36, no. 3, pp. 802–814, Mar. 2017.
14. D. Ardila, A. P. Kiraly, S. Bharadwaj, B. Choi, J. J. Reicher, L. Peng, D. Tse, M. Etemadi, W. Ye, G. Corrado, D. P. Naidich, and S. Shetty, ‘‘End-to-end lung cancer screening with three-dimensional deep learning on low-dose chest computed tomography,’’ Nature Med., vol. 25, no. 6, pp. 954–961, Jun. 2019.
15. S. Liu, A. Arindra Adiyoso Setio, F. C. Ghesu, E. Gibson, S. Grbic, B. Georgescu, and D. Comaniciu, ‘‘No surprises: Training robust lung nodule detection for low-dose CT scans by augmenting with adversarial attacks,’’ 2020, arXiv:2003.03824.
16. S. Zheng, J. Guo, X. Cui, R. N. J. Veldhuis, M. Oudkerk, and P. M. A. van Ooijen, ‘‘Automatic pulmonary nodule detection in CT scans using convolutional neural networks based on maximum intensity projection,’’ IEEE Trans. Med. Imag., vol. 39, no. 3, pp. 797–805, Mar. 2020.
17. G. Cao, T. Huang, K. Hou, W. Cao, P. Liu, and J. Zhang, ‘‘3D convolutional neural networks fusion model for lung nodule detection onClinical CT scans,’’ in Proc. IEEE Int. Conf. Bioinf. Biomed. (BIBM), Dec. 2018, pp. 973–978.
18. S. Zheng, J. Guo, X. Cui, R. N. J. Veldhuis, M. Oudkerk, and P. M. A. van Ooijen, ‘‘Automatic pulmonary nodule detection in CT scans using convolutional neural networks based on maximum intensity projection,’’ IEEE Trans. Med. Imag., vol. 39, no. 3, pp. 797–805, Mar. 2020.
19. S. G. and J. P., ‘‘A fully-automated system for identification and classification of subsolid nodules in lung computed tomographic scans,’’ Biomed. Signal Process. Control, vol. 53, Aug. 2019, Art. no. 101586.
20. F. Ciompi, K. Chung, S. J. van Riel, A. A. A. Setio, P. K. Gerke, C. Jacobs, E. T. Scholten, C. Schaefer-Prokop, M. M. W. Wille, A. Marchianá, U. Pastorino, M. Prokop, and B. van Ginneken, ‘‘Towards automatic pulmonary nodule management in lung cancer screening with deep learning,’’ Sci. Rep., vol. 7, no. 1, Apr. 2017, Art. no. 46479.
21. Ganesh, D., et al. "Implementation of AI Pop Bots and its allied Applications for Designing Efficient Curriculum in Early Childhood Education." International Journal of Early Childhood 14.03: 2022.
22. Kumar, M. Sunil, et al. "Deep Convolution Neural Network Based solution for Detecting Plant Diseases." Journal of Pharmaceutical Negative Results (2022): 464-471.
23. P. Sai Kiran. "Power aware virtual machine placement in IaaS cloud using discrete firefly algorithm." Applied Nanoscience (2022): 1-9.
24. Kumar, T. P., & Kumar, M. S. (2021). Optimised Levenshtein centroid cross-layer defence for multi-hop cognitive radio networks. IET Communications, 15(2), 245-256.
25. Natarajan, V. Anantha, et al. "Segmentation of nuclei in histopathology images using fully convolutional deep neural architecture." 2020 International Conference on computing and information technology (ICCIT-1441). IEEE, 2020.
26. Sangamithra, B., P. Neelima, and M. Sunil Kumar. "A memetic algorithm for multi objective vehicle routing problem with time windows." 2017 IEEE International Conference on Electrical, Instrumentation and Communication Engineering (ICEICE). IEEE, 2017.
27. Sunil Kumar, M., and A. Rama Mohan Reddy. "An Efficient Approach for Evolution of Functional Requirements to Improve the Quality of Software Architecture." Artificial Intelligence and Evolutionary Computations in Engineering Systems. Springer, New Delhi, 2016. 775-792.
28. Natarajan, V. Anantha, et al. "Prediction Of Soil Ph From Remote Sensing Data Using Gradient Boosted Regression Analysis." Journal of Pharmaceutical Negative Results (2022): 29-36.

29. Kumar, M. Sunil, et al. "APPLYING THE MODULAR ENCRYPTION STANDARD TO MOBILE CLOUD COMPUTING TO IMPROVE THE SAFETY OF HEALTH DATA." Journal of Pharmaceutical Negative Results (2022):
30. Prasad, Tvs Gowtham, et al. "Cnn Based Pathway Control To Prevent Covid Spread Using Face Mask And Body Temperature Detection." Journal of Pharmaceutical Negative Results (2022): 1374-1381.1911-1917.
31. Natarajan, V.A., Kumar, M.S., Patan, R., Kallam, S. and Mohamed, M.Y.N., 2020, September. Segmentation of nuclei in histopathology images using fully convolutional deep neural architecture. In 2020 International Conference on computing and information technology (ICCIT-1441) (pp. 1-7). IEEE.
32. Y. Balagurunathan, M. B. Schabath, H. Wang, Y. Liu, and R. J. Gillies, ‘‘Quantitative imaging features improve discrimination of malignancy in pulmonary nodules,’’ Sci. Rep., vol. 9, no. 1, Dec. 2019, Art. no. 8528.
33. M. Al-Shabi, H. K. Lee, and M. Tan, ‘‘Gated-dilated networks for lung nodule classification in CT scans,’’ IEEE Access, vol. 7, pp. 178827–178838, 2019.
34. W. Zhu, C. Liu, W. Fan, and X. Xie, ‘‘DeepLung: Deep 3D dual path nets for automated pulmonary nodule detection and classification,’’ in Proc. IEEE Winter Conf. Appl. Comput. Vis. (WACV), Mar. 2018, pp. 673–681.
35. N. Nasrullah, J. Sang, M. S. Alam, M. Mateen, B. Cai, and H. Hu, ‘‘Automated lung nodule detection and classification using deep learning combined with multiple strategies,’’ Sensors, vol. 19, no. 17, p. 3722, Aug. 2019.
36. J. L. Causey, J. Zhang, S. Ma, B. Jiang, J. A. Qualls, D. G. Politte, F. Prior, S. Zhang, and X. Huang, ‘‘Highly accurate model for prediction of lung nodule malignancy with CT scans,’’ Sci. Rep., vol. 8, no. 1, Jun. 2018, Art. no. 9286.
37. Y. Xie, Y. Xia, J. Zhang, Y. Song, D. Feng, M. Fulham, and W. Cai, ‘‘Knowledge-based collaborative deep learning for benign-malignant lung nodule classification on chest CT,’’ IEEE Trans. Med. Imag., vol. 38, no. 4, pp. 991–1004, Apr. 2019.
38. Jakhar, S.P., Nandal, A., Dixit, R. (2021). Classification and Measuring Accuracy of Lenses Using Inception Model V3. In: Sharma, M.K., Dhaka, V.S., Perumal, T., Dey, N., Tavares, J.M.R.S. (eds) Innovations in Computational Intelligence and Computer Vision. Advances in Intelligent Systems and Computing, vol 1189. Springer, Singapore.
39. Yashowardhan Shinde. (2021, August 26). “How to code your ResNet from scratch in Tensorflow?”. https://www.analyticsvidhya.com/blog/2021/08/how-to-code-your-resnet-from-scratch-in-tensorflow/
40. Vaibhav Khandelwal. (2020, August 17). “The Architecture and Implementation of VGG-16” https://pub.towardsai.net/the-architecture-and-implementation-of-vgg-16-b050e5a5920b.